IABSE Symposium 2025
Environmentally Friendly Technologies and Structures - Focusing on Sustainable Approaches
May 18-21, 2025 | Tokyo, Japan

Seismic Fragility Assessment using Explainable Deep Kernel Learning Surrogate Model considering Structural and Seismic Uncertainties

Taisei Saida, Mayuko Nishio

University of Tsukuba, Ibaraki, Japan

Contact: saida.taisei.tj@alumni.tsukuba.ac.jp

Abstract

This study proposes a surrogate model using deep kernel learning (DKL) with a convolutional neural network (CNN) and attention mechanism for efficient seismic fragility assessment of infrastructure. The CNN extracts features from seismic response spectrum, enabling efficient Gaussian process (GP) regression in a lower-dimensional space. An automatic relevance determination (ARD) kernel and attention mechanism enhance explainability by evaluating input variable contributions and attention weights for response spectrum. The model achieved high prediction accuracy, outperforming GPs, especially with limited data. Fragility analysis using the surrogate model reduced computational cost to 0.05% of direct numerical simulation.

Keywords: Seismic Response, Reliability Analysis, Explainablity, Fragility Analysis, Surrogate Model

1 Introduction

Unexpected earthquakes can cause significant damage to existing civil structures, such as bridges in road networks. Therefore, the seismic fragility assessment of these structures needs to be performed with lower computational cost. This assessment involves uncertainties in both the material properties of the structure (e.g., stiffness and mass) and the characteristics of the seismic loading. However, performing calculations that consider these uncertainties requires a vast number of repeated analyses to explore the combinations of uncertain parameters. These iterative calculations become computationally prohibitive, especially when dealing with seismic response analyses. Consequently, surrogate models based on machine learning is a promising approach to replace seismic response analyses.

A surrogate model is a machine learning-based regression model where uncertain parameters serve as inputs, and structural responses are the outputs. Since Bucher and Bourgund [1] introduced response surface method for reliability analysis, various methods, including artificial neural networks and support vector regression, have been proposed. Gaussian Process (GP) [2] is also commonly used for surrogate modeling. GP offer several advantages: they can provide predictive variance and are robust against overfitting.

In the context of seismic response analysis, seismic loads introduce significant uncertainty that must be addressed. A key challenge is that seismic loads are time-history data, representing high-dimensional features. Directly inputting these high-dimensional features into a GP surrogate model can lead to the "curse of dimensionality," [3] potentially causing a drastic decrease in accuracy.

Therefore, dimensionality reduction methods are preferable before the GP model. One approach for dimensionality reduction is to use intensity measures (IM) of the seismic load, such as peak ground acceleration (PGA) or spectral acceleration (Sa), as inputs. However, this method may not fully capture the characteristics of the high-dimensional ground motion. Another approach uses autoencoders (AE) or principal component analysis (PCA), subsequently feeding these features into a GP. While this reduces the dimensionality of seismic load features, a limitation is that AE and PCA are not designed to optimize the extracted features for the subsequent GP regression.

To address these limitations, this study proposes a surrogate model based on deep kernel learning (DKL) [4], which combines a deep neural network with a GP. DKL maps high-dimensional input data into a low-dimensional latent space using a deep neural network, and then performs regression using a GP in this latent space. The deep neural network is expected to automatically learn features from the input data for the regression task, while the GP provides nonlinear regression using these low-dimensional features. In the proposed DKL surrogate model, response spectrum data of the seismic load is first input into the deep neural network, which outputs low-dimensional features. These features are expected to include the crucial information influencing the structural response. Subsequently, these low-dimensional features, along with the uncertain structural parameters, are used as inputs to the GP to predict the structural response. During the DKL training process, the deep neural network and the GP are optimized simultaneously, ensuring that the extracted features are optimized for the GP regression. Furthermore, this study addresses the issue of explainability in the context of validating surrogate models. In numerical analysis, verifying the validity of the analysis results is essential for their appropriate use. This requirement naturally extends to surrogate models, necessitating the ability to assess the reliability of their predictions. This is particularly important because surrogate models are often built using machine learning techniques, which are "black boxes." Blindly accepting their predictions can be risky, especially for critical infrastructure, where incorrect predictions can have significant consequences. Therefore, this study focuses on explainability, which aims to reveal which aspects of the input data a machine learning model focuses on to arrive at its predictions. By examining these points of focus, engineers can assess whether the model align with engineering knowledge and judge its validity.

This study addresses the issue of explainability by employing a DKL with an automatic relevance determination (ARD) kernel function and an attention mechanism. The ARD kernel function, a kernel function that can assign a length-scale to each input variable, enables the quantification of the contribution of each input variable. An attention mechanism [5] assigns weights to different elements of the input data, thereby indicating their relative importance. By integrating this attention mechanism into the feature extraction process from response spectrum using a convolutional neural network (CNN), the aim is to capture which frequency components of the input response spectrum are emphasized during the extraction of low-dimensional features. Specifically, attention weights are applied to the output layer of the CNN, corresponding to each frequency in the input response spectrum. This explainable modeling approach allows for the quantitative assessment of the significance of structural parameters and frequency components within the response spectrum. These emphasized features provides insights such as the following. If high attention weights are assigned to frequency components near the modal frequencies of the structure, this suggests that the surrogate model is capturing the underlying physics of seismic response, indicating its potential validity.

2 Deep Kernel Learning with Attention Mechanism

The DKL model developed in this study is described in this section along with its formulation. In addition, multi-output GP is utilized for the scenarios with multiple structural outputs. The approach to explainability, facilitated by the ARD kernel and attention mechanism, is also described.

2.1 Gaussian Process Regression

First, consider a training dataset $\mathcal{D}^{\text{train}}$ comprising input-output pairs $(\mathbf{x}, y)$:

$$\mathcal{D}^{\text{train}} = \{(\mathbf{x}_1, y_1), (\mathbf{x}_2, y_2), \dots, (\mathbf{x}_n, y_n)\}$$
$$\text{where } \mathbf{x}_i = (\mathbf{x}_i^{\text{struct}}, \mathbf{x}_i^{\text{seismic}}), i = 1,2,\dots,n \quad (1)$$

Here, *n* represents the number of training data points, $\mathbf{x}_i^{\text{struct}}$ denotes the structural uncertainty parameters, and $\mathbf{x}_i^{\text{seismic}}$ represents the seismic response spectrum. It is assumed that the relationship between y and $\mathbf{x}$ can be described by a function f:

$$y = f(\boldsymbol{x}) \quad (2)$$

It is assumed that y is standardized to have a zero mean, and f follows a Gaussian process with a zero mean function, expressible as:

$$f \sim \mathcal{GP}\left(0, k(\mathbf{x}_i, \mathbf{x}_j)\right) \quad (3)$$

where k is the kernel function. Utilizing this kernel function, the elements K_{ij} of the kernel matrix $\mathbf{K}$ are calculated as follows:

$$K_{ij} = k(\mathbf{x}_i, \mathbf{x}_j) \quad (4)$$

The Matern 5/2 kernel is utilized as the base kernel function in this study, defined as:

$$k(\mathbf{x}_i, \mathbf{x}_j) = \sigma^2 \left(1 + \sqrt{5}r + \frac{5}{3}r^2\right) exp(-\sqrt{5}r)$$
$$\text{where } r(\mathbf{x}_i, \mathbf{x}_j) = \sqrt{\sum_{k=1}^{L} \frac{(x_{ik} - x_{jk})^2}{l_k^2}} \quad (5)$$

Here, L is the dimensionality of the input parameters and l_k is the hyperparameter called the length-scale. This parameter controls the sensitivity of the kernel to changes in the k-th input dimension. A smaller value of l_k indicates that the kernel is highly sensitive to variations in the corresponding input parameter, implying a greater influence of that parameter on the output. To evaluate the contribution of each parameter, an index c_k was defined. This index transforms the length-scale l_k into a relative percentage contribution for each input dimension k, and is defined as follows:

$$c_k = \frac{1/l_k}{\sum_{m=1}^{L}(1/l_m)} \quad (6)$$

2.2 Multi-Output Gaussian Process Regression

Multi-output GP regression, proposed by Bonilla et al. [6], is a GP model capable of modeling correlations among outputs. Previous study by Saida et al. [7] has demonstrated the effectiveness of considering these correlations for structural responses. Consider a training dataset $\mathcal{D}^{\text{train multi}}$ comprising input $\mathbf{x}$ and output vector $\mathbf{y}$:

$$\mathcal{D}^{\text{train multi}} = \{(\mathbf{x}_1, \mathbf{y}_1), (\mathbf{x}_2, \mathbf{y}_2), \dots, (\mathbf{x}_n, \mathbf{y}_n)\}$$
$$\text{where } \mathbf{y}_i = [y_{i1}, y_{i2}, \dots, y_{im}]^T, i = 1,2,\dots,n \quad (7)$$

Here, m is the number of output variables. The approach by Bonilla et al., adopted in this study, efficiently models the covariance function of the multi-output GP through the use of a separable kernel structure. Specifically, $\mathbf{K}^{\text{multi}}$ is expressed using the Kronecker product of an output kernel $\mathbf{K}_{\text{o}}$ and an input kernel k_{x}:

$$\mathbf{K}^{\text{multi}}(\mathbf{x}_i, \mathbf{x}_j) = \mathbf{K}_{\text{o}} \otimes k_{\text{x}}(\mathbf{x}_i, \mathbf{x}_j) \quad (8)$$

Here, $\mathbf{K}_{\text{o}}$ is an $m \times m$ output covariance matrix that captures the dependencies between the outputs. For instance, the (p, q) element of $\mathbf{K}_{\text{o}}$ represents the covariance between output p and output q . k_{x} represents the input covariance function, for which the Matern 5/2 kernel function.

2.3 Deep Kernel Learning for Multi-Output Gaussian Process Regression

This section details the extension of multi-output GP to DKL [4]. This involves substituting the input kernel function $k_{\text{x}}(\mathbf{x}_i, \mathbf{x}_j)$ with a kernel function defined within a latent space learned by a deep neural network (DNN). Specifically, a Convolutional Neural Network (CNN) is used to map the seismic response spectrum $\mathbf{x}_i^{\text{seismic}}$ to a lower-dimensional latent representation $\mathbf{z}_i^{\text{seismic}}$:

$$\boldsymbol{z}_i^{\text{seismic}} = \text{DNN}(\mathbf{x}_i^{\text{seismic}}) \quad (9)$$

where DNN represents the mapping by DNN. The input kernel function in DKL, $k_{\text{x}}^{\text{DKL}}$, is defined using this latent representation:

$$k_{\text{x}}^{\text{DKL}}(\mathbf{x}_i, \mathbf{x}_j) = k_{\text{base}}\left(\phi(\mathbf{x}_i), \phi(\mathbf{x}_j)\right) \quad (10)$$

where k_{base} is the base kernel function (e.g., the Matern 5/2 kernel), and $\phi(\mathbf{x}_i) =$

$[\mathbf{x}_i^{\text{struct}\,T}, \mathbf{z}_i^{\text{seismic}\,T}]^T$ represents the feature mapping obtained by concatenating the structural uncertainty parameters and the latent representation. The covariance function for multi-output DKL is subsequently given by:

$$\mathbf{K}^{\text{multi DKL}}(\mathbf{x}_i, \mathbf{x}_j) = \mathbf{K}_{\text{o}} \otimes k_{\text{x}}^{\text{DKL}}(\mathbf{x}_i, \mathbf{x}_j) \quad (11)$$

The learning process for multi-output DKL involves the simultaneous optimization of the parameters of the kernel function, and the network parameters of the CNN, based on the log-likelihood. The multi-output DKL was implemented using GPyTorch [8], and Adam optimizer [9] was used for optimization.

2.4 Convolutional Neural Network with Attention Mechanism

As explained in Section 2.3, this study employs a CNN to extract features. While CNNs typically operate as black boxes, this study addresses this issue by integrating an attention mechanism [5] into the CNN. By applying weighted attention at the final layer of the CNN, it becomes possible to identify the dominant frequencies of the seismic response spectrum. Initially, the CNN extracts features as follows:

$$\mathbf{Z}_i^{\text{seismic cnn}} = \text{CNN}(\boldsymbol{x}_i^{\text{seismic}}) \quad (12)$$

This feature map, $\mathbf{Z}_i^{\text{seismic cnn}}$, is a matrix with dimensions corresponding to the number of output channels of the CNN and the frequency length of the seismic response spectrum (which is slightly reduced from the initial length due to the CNN). Global Average Pooling (GAP) is then applied along the output channel dimension of this feature map:

$$\mathbf{z}_i^{\text{seismic gap}} = \text{GAP}(\mathbf{Z}_i^{\text{seismic cnn}}) \quad (13)$$

This GAP operation reduces the feature map $\mathbf{Z}_i^{\text{seismic cnn}} \in \mathbb{R}^{C \times T'}$ to a feature vector $\mathbf{z}_i^{\text{seismic gap}} \in \mathbb{R}^{T'}$, where C is the number of output channels of the CNN and T' is the frequency length. Based on this $\mathbf{z}_i^{\text{seismic gap}}$, attention weights are calculated using a MLP as follows:

$$\boldsymbol{\alpha}_i = \text{Sigmoid}\left(\text{MLP}(\mathbf{z}_i^{\text{seismic gap}})\right) \quad (14)$$

Here, Sigmoid is the Sigmoid activation function, and MLP represents a mapping using MLP. The dimension of $\boldsymbol{\alpha}_i$ is the same as the length T' related to the frequency, assigning a weight to each frequency component of the feature map. These attention weights thus indicate the importance of each frequency component in the original feature map $\mathbf{Z}_i^{\text{seismic cnn}}$. Using these attention weights, the original feature map is weighted as follows:

$$\mathbf{Z}_i^{\text{seismic att}} = \mathbf{Z}_i^{\text{seismic cnn}} \odot \boldsymbol{\alpha}_i^T \quad (15)$$

where $\odot$ denotes element-wise multiplication, and $\boldsymbol{\alpha}_i$ is broadcast across the channel dimension to match the dimensions of $\mathbf{Z}_i^{\text{seismic cnn}}$. Subsequently, GAP is applied to this attention-weighted feature map:

$$\mathbf{z}_i^{\text{seismic att gap}} = \text{GAP}(\mathbf{Z}_i^{\text{seismic att}}) \quad (16)$$

A linear layer is applied to this vector to transform it into the latent vector used as input to the GP layer of the DKL model:

$$\mathbf{z}_i^{\text{seismic}} = \mathbf{W}\mathbf{z}_i^{\text{seismic att gap}} + \mathbf{b} \quad (17)$$

Here, $\mathbf{W}$ is the weight matrix and $\mathbf{b}$ is the bias vector of the linear layer. This linear transformation allows for final dimensionality modification of the features before the GP. The resulting vector $\mathbf{z}_i^{\text{seismic}}$ is the latent representation of the seismic response spectrum and is ready to be combined with the structural uncertainty parameters as described in Section 2.3.

3 Seismic Response Analysis of Seismic Isolated Bridge RC Pier

3.1 Numerical Modelling of Seismic Isolated Bridge Pier

The structure used for verifying the developed surrogate modeling approach is a seismic isolated concrete bridge pier, as presented in documents related to the seismic design of road bridges in Japan [10,11]. This bridge pier was modeled using a two-degree-of-freedom lumped mass system for nonlinear time history analysis under seismic loading. As shown in Figure 1, the superstructure and the RC pier were represented as lumped masses, while the seismic isolation bearing and the RC pier were represented by nonlinear springs. For the hysteresis of the nonlinear springs, a bilinear model was applied to the seismic isolation bearing, and the Takeda model [12] was applied to the RC

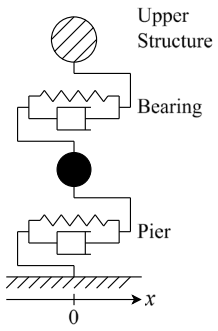

Figure 1. Two-degree-of-freedom model of a typical RC piers with a seismic rubber bearing

Table 1. Uncertain parameters in RC pier

Parameter		Nominal	Uncertainty (Uniform Distribution)
Seismic Isolation Bearing	Initial Stiffness (K_{B1})	4.0 × 10^7 (N/m)	±10 %
	Secondary Stiffness (K_{B2})	6.2 × 10^6 (N/m)	±10 %
	Yield Load (Q_B)	1.1 × 10^6 (N)	±10 %
Superstructure	Mass (M_U)	6.0 × 10^5 (kg)	±5 %
RC Pier	Mass (M_{RC})	3.5 × 10^5 (kg)	±5 %
	Initial Stiffness (K_{RC})	1.1 × 10^8 (N/m)	±7 %

pier. Table 1 lists the uncertain structural parameters of the model. Calculating the modal periods with nominal structural parameters yielded 0.919 seconds for the first mode and 0.297 seconds for the second mode. The time step for the analysis was set to 0.001 seconds, and the Newmark-beta method was used for numerical integration. For structural damping, Rayleigh damping with a damping coefficient of 0% for the seismic isolation bearing and 2% for the RC pier was assumed.

3.2 Seismic Load Selection

This study addresses the uncertainty in seismic ground motions through a process of ground motion sampling. The ground motion data were sourced from the K-NET and Kik-net strong-motion networks [13]. Initially, based on magnitude and focal distance, the ground motions were categorized into four distinct categories (LMSD: Large Magnitude-Short Distance, LMLD: Large Magnitude-Long Distance, SMSD: Small Magnitude-Short Distance, and Small Magnitude-Long Distance), as listed in Table 2. In addition, a Type 1 soil profile was specifically selected as the soil condition. Subsequently, for each of the categories, the ground motion selection methodology proposed by Baker [14] was implemented. This method samples ground motion under the assumption that the response spectrums follow a log-normal distribution. This process resulted in the selection of 50 waveforms per category, totaling 200 waveforms.

Table 2. Categories of Seismic Load Selection

Category	Magnitude (M)	Focal Distance (R, km)
LMSD	6.5 ≤ M < 7.5	10 < R ≤ 30
LMLD	6.5 ≤ M < 7.5	30 < R ≤ 60
SMSD	5.5 ≤ M < 6.5	10 < R ≤ 30
SMLD	5.5 ≤ M < 6.5	30 < R ≤ 60

3.3 Fragility Assessment

This study conducts a fragility analysis. For the fragility curves, a lognormal distribution function defined by Shinozuka et al. [15] is employed.

$$F_k(\delta_{resp}) = \int_0^{\delta_{resp}} \frac{1}{\sqrt{2\pi}\zeta_X} exp\left(-\frac{1}{2}\left(\frac{lnz - ln\delta_k}{\zeta_X}\right)^2\right) dz \quad (18)$$

Here, k denotes a specific damage state, δ_k represents the median capacity converted to response displacement, and ζ_X is the logarithmic standard deviation. By varying δ_{resp} from 0 to infinity according to the seismic intensity, the probability of exceeding the damage level corresponding to the limit state displacement δ_k is obtained. Eqn. (18) can be expressed using the standard normal distribution function as follows:

$$F_k(\delta_{resp}) = \Phi\left(\frac{ln(\delta_{resp}/\delta_k)}{\zeta_X}\right) \quad (19)$$

In this research, the acceleration response spectrum at the first modal period with a damping ratio of 0.05, $\mathrm{Sa}(T_1)$,is adopted as the ground motion intensity measure. Here, T_1 is the first modal period value. The damage state is defined as when the maximum displacement of the bridge pier exceeds the yield displacement. The yield displacement is set to 0.028 m. For the estimation of fragility parameters, the method of maximizing the following binomial likelihood L is utilized:

$$L(\alpha_i : c_m, \xi_Z) = \prod_{i=1}^{n} F_Z(\alpha_i : c_m, \xi_Z)^{q_i}(1 - F_Z(\alpha_i : c_m, \xi_Z)^{1-q_i}) \quad (20)$$

Here, q is a binary function that takes a value of 1 if damage occurs and 0 otherwise, α represents the applied ground motion, and n is the number of samples. The unknown quantities are the median capacity c_{m} and the composite logarithmic standard deviation ξ_{Z} , which accounts for the uncertainties in the ground motion and the capacity.

4 Results of DKL Surrogate Model Construction

This section presents the results of constructing the DKL surrogate model. To investigate the effect of the number of training data on the accuracy of the DKL surrogate model, an evaluation was performed using the coefficient of determination, R^2.

$$R^2 = \frac{\sum_{i=1}^{n}(y_i - \widehat{y_i})^2}{\sum_{i=1}^{n}(y_i - \bar{y})^2} \quad (21)$$

Here, y_i represents the true value, $\widehat{y_i}$ is the predicted value from the DKL surrogate model, $\bar{y}$ is the mean of the true values, and n is the number of data points. R^2 serves as an indicator with values closer to 1 indicating higher model accuracy. For each training data size, the surrogate model construction was performed five times, and the mean and variance of the results were evaluated. The total dataset comprised 1,000,000 data points (5,000 samples for structural parameter uncertainty × 200 seismic waveforms). Training data were sampled randomly, and the remaining data were used as the test data. For comparison, a GP model was employed. This GP model was formulated as a multi-output model described in Section 2.2, with structural parameters and IMs – specifically PGA, PGV, Alias Intensity, Sa(T_1), Sa(0.5), Sa(1.0), Sa(1.5), and Sa(2.0) – serving as inputs. To ensure consistent dimensionality of seismic load features with the GP model, the features of the DKL model were also compressed to 8 dimensions, enabling a comparison of accuracy between the two approaches: seismic load characterization using IMs and feature extraction via CNN.

Figure 2 illustrates the plotted R^2 values. Specifically, Figure 2. (a) presents the prediction results for the maximum displacement of the pier, and Figure 2. (b) displays the prediction results for the maximum relative displacement of the bearing. Observing Figure 2. (a), the R^2 value of the DKL surrogate model increases with the number of training data. Notably, in the region with a smaller number of training data, the DKL model achieves a higher R^2 value compared to the GP model, suggesting its ability to learn effectively even with limited data. Conversely, with a larger number of training data points, such as 400 or 500, the R^2 values of the DKL and GP models are almost equivalent. Similarly, Figure 2. (b) exhibits a generally similar trend to the maximum displacement of the pier. When the number of training data is small, the DKL model demonstrates a higher R^2 value than the GP model. As the number of training data increases, the R^2 value of the GP model improves and approaches that of the DKL model. These findings suggest that, particularly when the number of training data is limited, the features extracted by the CNN from the response spectra are more effective than IM-based features for predicting the maximum displacement of both the pier and the bearing. Then, the contribution derived from the length-scale of the ARD kernel, specifically c_k from Eqn. (6), is examined. To investigate this contribution, a DKL surrogate model trained on 500 data samples was utilized. A bar graph illustrating these c_k values is presented in Figure 3 The horizontal axis represents the contribution, while the vertical axis corresponds to the input variables of the GP. F1 through F8 denote the seismic spectrum features extracted by the CNN. Observation of this figure reveals a high contribution from the seismic motion-related features, F1 through F8. This suggests that variations in seismic motion characteristics exerted

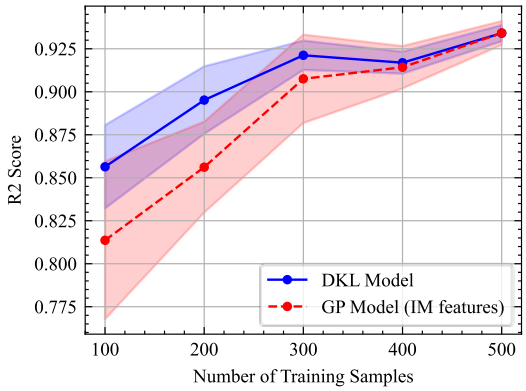

(a) Max Displacement of the Pier

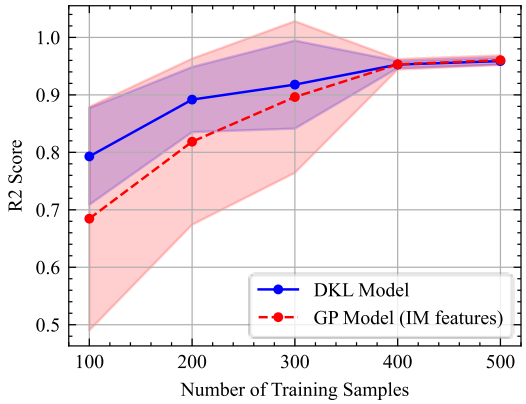

(b) Max Relative Displacement of the Bearing

Figure 2. Accuracy of DKL Surrogate Model

a greater influence on the output compared to variations in structural parameters. Among the structural parameters, K_{RC}, representing the initial stiffness parameter of the RC pier, exhibits the largest contribution. This indicates that variations in the stiffness of the RC pier significantly contributed to the maximum displacement, which is the output. Conversely, the parameter with the smallest contribution is Q_B, the yield load of bearing. Considering that this verification involved a wide range of seismic load categories as detailed in Table 2, and that not all calculated seismic responses necessarily reached the yield displacement, this result appears to be reasonable.

In addition, the contribution of individual frequency components of the response spectrum is examined based on the weights derived from the attention mechanism. To investigate this contribution, a DKL surrogate model trained on 500 data samples was employed. This contribution is visualized by color-coding the response spectrum

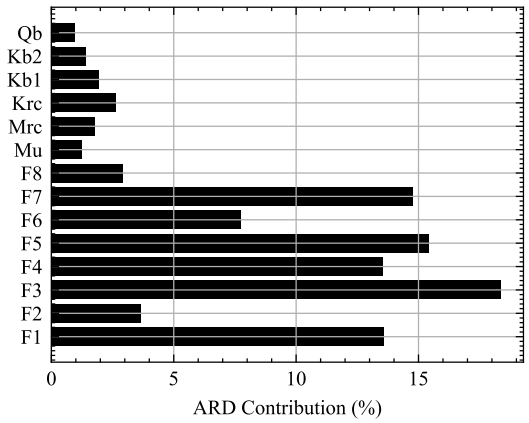

Figure 3. Estimated Contribution by ARD Kernel

according to the α values obtained from Eqn. (14). Examples of these color-coded response spectra are presented in Figure 4. (a) and (b). Here, red indicates a higher α value, signifying a greater contribution, while blue indicates a lower α value, signifying a smaller contribution. Observation of Figure 4. (a) reveals a significant contribution around 0.9 second and 0.3 seconds, corresponding to the modal periods of the RC bridge pier. This aligns with expectations based on structural engineering knowledge. Conversely, Figure 4. (b) shows a high contribution at frequency components unrelated to the modal periods. This is inconsistent with structural engineering knowledge. During this verification, instances similar to Figure 4. (b), where a high contribution is observed at frequencies unrelated to the modal period, were frequently encountered. Conversely, the DKL model exhibits high accuracy, with an R^2 value exceeding 0.9. The high DKL accuracy despite irrelevant frequency contributions suggests that small attention weights are not negligible in the GP, which has nature as an interpolation function. This highlights the need for different explainability approaches.

Finally, fragility curves are calculated using the DKL surrogate model. The DKL surrogate model employed here was constructed with 500 training data points. For the fragility curve calculation, the maximum displacement of the pier was predicted for 999,500 uncertainty sample points in the test data. Based on these predictions, fragility curves were calculated using the method described in Section 3.3. Figure 5 illustrates the calculated fragility curves. In this figure, the black line

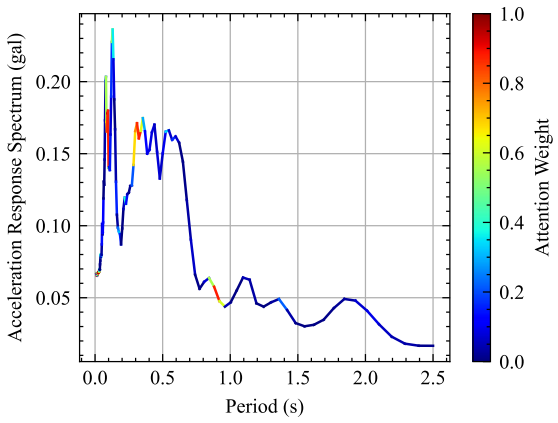

(a) Case of high acceptability

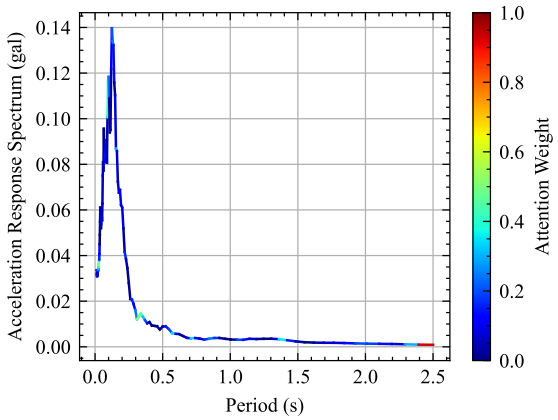

(b) *Case of low acceptability*

Figure 4. Estimated Seismic Load Contribution by Attention Mechanism

represents the fragility curve obtained using the surrogate model, and the red dashed line represents the fragility curve derived from numerical analyses using the Monte Carlo method. The horizontal axis represents Sa(T_1), and the vertical axis represents the probability of failure. As shown in the figure, the surrogate model and numerical analysis results exhibit agreement in the lower Sa(T_1) range (Sa(T_1) < 250 gal). However, the disagreement becomes apparent in the range over 250 gal, with the surrogate model predicting higher failure probabilities compared to those by the numerical analysis. This is because the selected seismic waveforms for training based on the sampling method by Baker [14] was not appropriate as the training data. In detail, the uncertainty of seismic loads considered there has the distribution less frequencies in the range of high Sa(T_1) values than those in lower Sa(T_1).

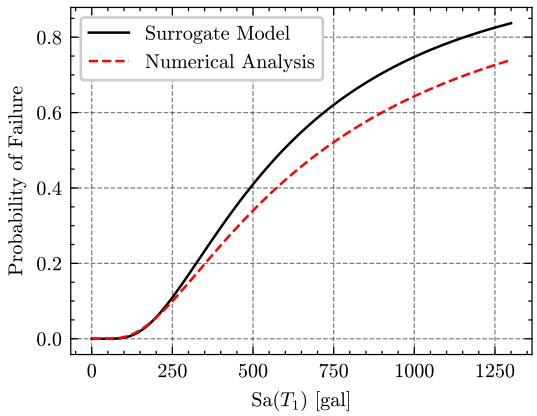

Figure 5. Fragility Curve using Surrogate Model Predictions

Nevertheless, the computational time exhibits a remarkable difference. The prediction using the surrogate model is negligibly small compared to the numerical analysis. Therefore, the computational cost associated with the surrogate model is solely the cost of the 500 numerical analyses used for its construction. In essence, the computational cost of calculating the fragility curve using the surrogate model is approximately 0.05% (= 500 / 999,500) of the computational cost required for calculating the fragility curve using numerical analysis with 999,500 Monte Carlo simulations, demonstrating a substantial reduction in computational cost. To address the fragility curve disagreement, training with a more uniform distribution of response spectrum could improve model generalization across the Sa(T_1) range. Moreover, adaptive sampling techniques, by focusing on data-sparse regions, especially at higher Sa(T_1), could further refine the training dataset. These refinements are expected to improve the accuracy of the surrogate model for fragility curve estimation.

5 Conclusions

This study proposes a surrogate model integrating DKL, a CNN, and an attention mechanism to reduce computational cost. The CNN facilitates feature extraction from seismic response spectrum, thereby enabling efficient GP regression in a reduced-dimensional space. Furthermore, the contributions of input variables and the importance of frequency components within the response spectrum are assessed through the

application of an ARD kernel and an attention mechanism, with the objective of improving model explainability.

The developed surrogate model demonstrated superior prediction accuracy over standard GP, particularly with limited training data. Analysis employing the ARD kernel indicated that features related to seismic motion had a more substantial influence on the output than variations in structural parameters. Additionally, while the attention mechanism highlighted the importance of frequency components around the structure's dominant frequencies, instances inconsistent with structural engineering knowledge were also observed, suggesting limitations in relying solely on the attention mechanism for complete explainability. Fragility analysis utilizing the proposed surrogate model demonstrated a significant reduction in computational cost, achieving a mere 0.05% of that required by Monte Carlo simulations based on numerical analysis.

Based on the results, the DKL surrogate model is deemed an effective methodology for achieving both high prediction accuracy and computational efficiency, thereby streamlining fragility analysis within the seismic performance evaluation of infrastructure. However, the explainability of the model warrants further investigation.

6 Acknowledgements

This study was supported by the Japan Society for the Promotion of Science (JSPS) KAKENHI [grant number 24KJ0474] and Japan Science and Technology Agency (JST) FOREST Program [grant number JPMJFR205T].

7 References

[1] Bucher CG, Bourgund U. A fast and efficient response surface approach for structural reliability problems. Struct Saf 1990;7:57–66.

[2] Williams CKI, Rasmussen CE. Gaussian processes for regression. Advances in Neural Information Processing Systems 1995.

[3] Bellman R. Dynamic programming. Science 1966;153:34–7.

[4] Wilson AG, Hu Z, Salakhutdinov R, Xing EP. Deep Kernel Learning. In: Gretton A, Robert CC, editors. Proceedings of the 19th International Conference on Artificial Intelligence and Statistics, vol. 51, Cadiz, Spain: PMLR; 09--11 May 2016, p. 370–8.

[5] Vaswani A, Shazeer N, Parmar N, Uszkoreit J, Jones L, Gomez AN, et al. Attention is all you need. vol. 30, proceedings.neurips.cc; 2017.

[6] Bonilla EV, Chai K, Williams C. Multi-task Gaussian Process Prediction. Adv Neural Inf Process Syst 2007;20.

[7] Saida T, Rashid M, Nishio M. System fragility analysis of highway bridge using multi-output Gaussian process regression surrogate model. Adv Struct Eng 2024;27:2803–22.

[8] Gardner JR, Pleiss G, Bindel D, Weinberger KQ, Wilson AG. GPyTorch: Blackbox Matrix-matrix Gaussian process inference with GPU acceleration. Advances in Neural Information Processing Systems, vol. 31, Curran Associates, Inc.; 2018.

[9] Kingma DP, Ba J. Adam: A Method for Stochastic Optimization. ArXiv [CsLG] 2014.

[10] Japan Road Association. Handouts on Seismic Design of Road Bridges [Translated from Japanese]. Japan Road Association; 1997.

[11] Japan Road Association. SPECIFICATIONS FOR HIGHWAY BRIDGES Part V SEISMIC DESIGN. Japan Road Association; 2016.

[12] Takeda T, Sozen MA, Nielsen NN. Reinforced Concrete Response to Simulated Earthquakes. Journal of the Structural Division 1970;96:2557–73.

[13] National Research Institute for Earth Science and Disaster Resilience. NIED K-NET, KiK-net 2019. https://doi.org/10.17598/NIED.0004.

[14] Baker JW, Lin T, Shahi SK, Jayaram N. New ground motion selection procedures and selected motions for the PEER transportation research program. PEER Report 2011.

[15] Shinozuka M, Feng MQ, Lee J, Naganuma T. Statistical analysis of fragility curves. J Eng Mech 2000;126:1224–31.